The Complex Phase Lag Behavior of the 3–12 Hz Quasi-Periodic Oscillations during the Very High State of XTE J1550–564

Rudy Wijnands[1], Jeroen Homan, & Michiel van der Klis

Astronomical Institute "Anton Pannekoek", University of Amsterdam, and Center for High Energy Astrophysics, Kruislaan 403, NL-1098 SJ Amsterdam, The Netherlands;

rudy@astro.uva.nl, homan@astro.uva.nl, michiel@astro.uva.nl

Received _____; accepted _____

Accepted for publication in ApJ Letters, 29 September 1999

[1]Chandra Fellow. Present address: Center for Space Research, MIT, Cambridge, MA 02139, USA

ABSTRACT

We present a study of the complex phase lag behavior of the low-frequency (<20 Hz) quasi-periodic oscillations (QPOs) in the X-ray transient and black-hole candidate XTE J1550–564 during its very high state. We distinguish two different types of low-frequency QPOs, based on their coherence and harmonic content. The first type is characterized by a 6 Hz QPO with a Q (the QPO frequency divided by the QPO width) of < 3 and with a harmonic at 12 Hz. The second type of QPO is characterized by a 6 Hz QPO with a Q value of > 6 and with harmonics at 3, 12, 18, and possibly at 9 Hz. Not only the Q values and the harmonic content of the two types are different, but also their phase lag behavior. For the first type of QPO, the low energy photons (<5 keV) of both the 6 Hz QPO and its harmonic at 12 Hz lag the hard energy photons (>5 keV) by as much as 1.3 radian. The phase lags of the second type of QPO are more complex. The soft photons (< 5 keV) of the 3 and the 12 Hz QPOs *lag* the hard photons (> 5 keV) by as much as 1.0 radian. However, the soft photons of the 6 Hz QPO *precede* the hard ones by as much as 0.6 radian. This means that different harmonics of this type of QPO have different signs for their phase lags. This unusual behavior is hard to explain when the lags are due to light-travel-time differences between the photons at different energies, e.g., in a Comptonizing region surrounding the area where the QPOs are formed.

Subject headings: accretion, accretion disks — stars: individual (XTE J1550–564) — stars: neutron — X-rays: stars

1. Introduction

The soft X-ray transient and black-hole candidate XTE J1550–564 was discovered early September 1998 (Smith 1998) with the All Sky Monitor on board the *Rossi X-ray Timing Explorer* (*RXTE*). Subsequent observations with the *RXTE* Proportional Counter Array during the initial rise, showed 0.08–4 Hz quasi-periodic oscillations (QPOs) in the power spectrum, superimposed on strong (∼30% rms amplitude) band-limited noise (Cui et al. 1999). On 19–20 September 1998, a strong X-ray flare was detected with a peak luminosity of ∼6.5 Crab (Remillard et al. 1998). During this flare, QPOs near 185 Hz were discovered (McClintock et al. 1998; Remillard et al. 1999) simultaneously with low-frequency (<20 Hz) QPOs, strongly indicating that XTE J1550–564 was in the very high state (VHS) during these observations. The X-ray spectral properties and the rapid X-ray variability during the first part of the outburst were discussed by Cui et al. (1998), Sobczak et al. (1999), and Remillard et al. (1999). A second VHS episode began on March 4 1999, when QPOs near 280 and 6 Hz were detected (Homan, Wijnands, & van der Klis 1999a). These QPOs and the other rapid X-ray variability will be discussed by Homan et al. (1999b). In this *Letter*, we concentrate on the small subset of the observations discussed by Homan et al. (1999b) when XTE J1550–564 was in the VHS, showing QPOs above 100 Hz and around 6 Hz. We report on the very complex phase lag behavior of the low-frequency QPOs.

2. Observation and selection method

Our primary goal is to study the phase lag behavior of the low-frequency QPOs when XTE J1550–564 was in the 1999 VHS episode (see Homan et al. 1999b). The public *RXTE* observations used are listed in Table 1. Data were accumulated in several different observational modes, which were simultaneously active. We used the 'Binned' mode data, with a time resolution of 4 ms in 8 photon energy bands (covering 2–13.1 keV), and the

'Event' mode data, with a time resolution of 16 μs in 16 bands (13.1–60 keV). To determine the QPO properties, we calculated power and cross spectra using 16 or 256-s intervals and a Nyquist frequency of 128 Hz. To correct for the dead-time effects on the lags, we subtracted the average 50–125 Hz cross-vector from the cross spectra (see van der Klis et al. 1987).

The VHS observations can be divided according to the properties of the QPOs below 20 Hz. We distinguish two types based on the Q value (frequency divided by FWHM) of the 6 Hz QPO[2], and its harmonic structure: one type with a relatively broad (Q $<$ 3) 6 Hz QPO with a harmonic at 12 Hz (type A QPOs; § 3; Fig. 1*a*), and no other detectable harmonics, and one with a relatively narrow (Q $>$ 6) 6 Hz QPO with harmonics at 3, 12, 18 (although not always detectable due to the limited statistics), and possibly at 9 Hz (type B QPOs; § 4; Fig. 1*b*). The observations are listed in Table 1 according to the type of QPO they contain. Although the power spectra of the 40401-01-57-00 and 40401-01-58-01 observations show fewer harmonics and stronger band-limited noise, these observations are classified as containing type B QPOs because of the high Q ($>$ 6) values of the 6 Hz QPOs.

3. Type A low-frequency QPOs

Figure 1*a* shows a typical power spectrum (i.e., for observation 40401-01-50-00) containing type A QPOs. Clearly visible is the 6 Hz QPO with a shoulder at higher frequencies. When using the data combined for the total *RXTE* energy range (effectively 2–60 keV) and fitting the data with two Lorentzian or two Gaussian functions, the frequency of the second QPO is not twice the frequency of the 6 Hz QPO. The ratio between the frequency of the second QPO and the frequency of the 6 Hz QPO is 1.5–1.8 (depending on

[2]Although the frequency of this QPO varied between 5 and 7 Hz, for reasons of clarity this QPO will be referred to as the '6 Hz QPO'.

observation and on the fit function [Lorentzian or Gaussian]). Fitting the total energy band power spectrum with two QPO functions which are harmonically related to each other, results in fits which are unacceptable. However, by using only the data in the range 13.1–48 keV (or 8.0–48 keV when the statistics did not allow to detect the 12 Hz QPO in the 13.1–48 keV range), the 6 Hz QPO is only marginally detectable and the most pronounced QPO is the 12 Hz QPO. The ratio between its frequency and that of the 6 Hz QPO (1.91–2.06; depending on observation) indicates that a harmonic relation with the 6 Hz QPO is likely. Clearly, the structure of the power spectrum is more complex than two harmonically related QPOs. Either the QPO shapes are more complex than Lorentzian or Gaussian functions, or an extra noise component (maybe a QPO) is present between the two QPOs.

A typical phase lag spectrum (i.e., for observation 40401-01-50-00) calculated between 2.5–6.5 and 6.5–48.0 keV is shown in Figure 1*c*. It can clearly be seen that in the frequency range 6–12 Hz, the soft photons (< 6.5 keV) lag the hard ones (> 6.5 keV) by $\sim$0.3 radian. Negative lags mean that the soft photons arrive later than the hard ones (a soft lag). The phase lag of the power law noise component below 1 Hz was consistent with being zero (0.03 ± 0.04 radian for the frequency range 0.01–1 Hz). An extrapolation of the phase lags (assuming a constant phase lag) of this noise component into the QPO frequency range cannot explain the phase lags observed for the QPOs. The lags determined for the QPOs must therefore be intrinsic to the QPOs. In the phase lag spectrum, the QPOs cannot be distinguished from each other or from the possible extra noise component in between them. Therefore, any interpretation of the QPO lags should be performed with caution.

In order to determine the phase lags as a function of photon energy, the frequency and the FWHM of both QPOs are needed. We decided to determine the frequency and FWHM of the 6 Hz QPO by fitting a Gaussian function in the total energy band. A Gaussian function fitted slightly better than a Lorentzian, although both functions yielded acceptable

fits. Because the type B QPOs need to be fitted with Gaussian functions in order to obtain acceptable fits (§ 4), we decided, for consistency, to use also Gaussian functions for the type A QPOs (note that a Gaussian function will result in a somewhat smaller FWHM than a Lorentzian function). After determining the properties of the 6 Hz QPO (FWHM 2–5 Hz; frequency 5.2–6.0 Hz) by using the full energy range, we determined the FWHM (2.5–10 Hz) of the 12 Hz QPO in the energy range above 8.0 or 13.1 keV by fixing its frequency to twice the 6 Hz QPO frequency. Usually, the fits were acceptable, although broad excess noise was sometimes present under the 12 Hz QPO. When including an extra component in the fit to account for this noise, the FWHM of the 12 Hz QPO was not significantly altered.

Using the thus obtained QPO parameters, we determined the frequencies and the FWHM of the QPOs for the different type A observations. We determined the phase lags between different energy ranges by calculating the average lags in the frequency range determined by the QPO FWHM centered on the QPO frequency. As a reference band, we used the 4.4–5.1 keV band. Figure 2*a* shows the phase lags as a function of photon energy for observation 40401-01-50-00. The soft photons (<5 keV) of the 6 Hz QPO (*open squares*) lag the hard ones (>5 keV) by ∼1.3 radian; the soft photons of the 12 Hz QPO (*open triangles*) lag the hard ones by ~ 0.6 radian (they are $< 3\sigma$ different from the 6 Hz QPO lags). The 6 Hz QPO lags in all the other observations with type A QPOs were consistent with these lags. Due to limited statistics, the 12 Hz QPO lags could only significantly be determined for observations 40401-01-50-00 and 40401-01-51-00. The measured lags and the upper limits obtained for the other observations were consistent with each other.

4. Type B low-frequency QPOs

Figure 1*b* shows a typical power spectrum (i.e, for observation 40401-01-53-00) containing type B low-frequency QPOs. Clearly visible is the very significant ($> 50\sigma$) 6

Hz QPO (with Q > 6) and those near 3, 12, and 18 Hz. The 3 Hz QPO seems to be the fundamental. Between the 6 and 12 Hz QPOs excess noise near 9 Hz is present, possibly due to another harmonic. A typical phase lag spectrum is shown in Figure 1*d* (calculated between 2.5–6.5 and 6.5–48.0 keV). Owing to the fact that the QPOs are relatively narrow, the individual components in the phase lag spectrum can more easily be distinguished than for the type A QPOs. Most striking is the fact that the 3 and 12 Hz QPO have *soft* lags (meaning that the photons below 6.5 keV arrive later than the ones above 6.5 keV) of 0.3–0.4 radian, whereas the 6 Hz QPO has a *hard* lag of 0.3 radian. Thus, the lags in the different QPO harmonics have different signs.

The power law noise between 0.01–0.5 Hz had a marginally significant soft lag of 0.05±0.02 radian. Above 0.5 Hz the lag increased (and became significant) to about 0.23±0.03 radian between 1 and 2.5 Hz. This is the frequency range where an extra noise component between 1 and 3 Hz is present, indicating that the observed lags in this frequency range are most likely those for this extra noise component and not for the power law noise. The above reported lag for the 3 Hz QPO could also be (partly) due to the lag of this extra noise component, but it is difficult to disentangle the two components. Clearly, an extrapolation of the soft lags (assuming a constant phase lag) below 3 Hz into the 6 Hz QPO frequency range cannot explain the hard lags observed for this QPO.

To determine the frequencies and the FWHM of these QPOs, we fitted the power spectra with several Gaussian functions (one for each QPO) that were harmonically related (using Lorentzians functions resulted in unacceptable fits). By including a power law function for the noise component below 1 Hz, and two extra Gaussians to fit the excess noise at 9 Hz and the noise between 1 and 3 Hz, we obtained acceptable fits with $\chi^2_{\rm red} \sim 1$. In this way, we obtained the frequencies and FWHMs of the various QPO harmonics. We determined the phase lags of the 3, 6, and 12 Hz QPOs in different energy ranges by

calculating the lags in a frequency range determined by the QPO FWHM centered on the QPO frequency. As a reference band we again used the 4.4–5.1 keV band. The statistics for the 18 Hz QPOs were not sufficient to allow detections of its lags. During some observations also the statistics of the other QPOs were not sufficient to allow significant detections.

A typical example of the resulting phase lags (i.e., for observation 40401-01-53-00) as a function of photon energy is shown in Figure 2*b*. The soft photons (<5 keV) of the 3 and 12 Hz QPOs *lag* the hard ones (>5 keV) by as much as 0.6 radian; the soft photons of the 6 Hz QPO *precede* the hard ones by about 0.6 radian. Again it is clearly visible that the phase lags of the different QPO harmonics have different signs. The QPO lags in the other observations with type B QPOs (except for observations 40401–01–57–00 and 40401–01–58–01, see below) were consistent with these lags, although for observation 40401–01–51–01 the hard lags of the 6 Hz QPOs were only 0.3 radian, i.e., half what is observed for the other observations (the soft lags in the 3 and 12 Hz QPOs during this observation are consistent with those obtained for the QPOs during the other observations).

The QPOs during the 40401–01–57–00 and 40401–01–58–01 observations do not follow the general type B picture. Their power spectra are shown in Figures 3*a* and *b*. During observation 40401–01–57–00, a strong band-limited noise is present, besides the type B QPOs (the Q is ∼6 and QPOs at 3 and 12 Hz are visible). The corresponding phase lag spectrum is shown in Figure 3*c*. Up to about 8 Hz the soft photons (below 6.5 keV) lag the hard ones (above 6.5 keV). Around 8–9 Hz a sudden jump in sign occurs and the lags become positive. The measured lags for these QPOs are likely a combination of the intrinsic QPO lags and the noise lags. The 3 Hz QPO phase lag is heavily affected by the lags of the underlying noise component; the 6 Hz QPO is also affected, though less than the 3 Hz QPO. Figure 2*c* shows the obtained phase lags versus photon energy for the different QPOs. Clearly, the lags measured in the frequency range of 3 and 6 Hz QPOs now have the

same sign: the soft photons *lag* the hard ones by 0.2 and 0.3 radian, respectively. However, the 12 Hz QPO now has a reversed sign: the soft photons *precede* the hard ones by ∼0.2 radian. This behavior is quite different from what is observed for the other type B QPOs.

During observation 40401–01–58–01, the source probably made a state transition within several minutes (see Homan et al. 1999b). We only used the data after this transition when two QPOs at 3 and 6 Hz were visible in the power spectrum (see Fig. 3*b*). An extra noise component in the same frequency range as the QPOs is visible. The phase lag spectrum of this observation is shown in Figure 3*d*. It is impossible to distinguish the 3 Hz QPO lag from that of the noise component. The combination of these two components results in a soft lag of ~ 0.2 radian. The 6 Hz QPO has hard lags. The absolute amplitude of its lag (~ 0.2 radian) is smaller than those of the other type B QPOs. This is most likely due to dilution by the broad band-limited noise component, which has soft lags. The phase lags of the two QPOs versus energy is shown in Figure 2*d*.

5. Discussion

We have presented the complex phase lag behavior of the low-frequency QPOs which are observed during the March 1999 VHS episode of XTE J1550–564. We distinguish two QPO types: one type with a relatively broad ($Q < 3$) 6 Hz QPO with a harmonic at 12 Hz, and one with a relatively narrow ($Q > 6$) 6 Hz QPO with harmonics at 3, 12, 18, and possibly at 9 Hz. The QPO phase lag behavior is different for both types. The first type always has soft lags, with a maximum amplitude of 0.6–1.3 radian. For the other type, the different harmonics have lags of different sign. The absolute maximum amplitude of the lags are also 0.6–1.3 radian. These phase lags are intrinsic to the QPOs. Extrapolation of the phase lags (assuming a constant phase lag) of the power law noise at frequencies lower than the QPO frequencies cannot explain the observed QPO lags. The noise lags are consistent

with zero, with upper limits of 0.06–0.15 radian, which is significantly lower than the QPO lags (0.6–1.3 radian). When an extra noise component (in addition to the power law noise) is present in the QPO frequency range, the phase lag behavior becomes more complex, but detailed studies of the lags are difficult due to the dilution by this noise component.

Our results show that the phase lag behavior of the low-frequency QPOs in XTE J1550–564 is quite complex. Especially the different signs for the lags of different harmonics are unexpected. This different sign strongly indicates that differences in light-travel time between the soft and hard photons cannot account for the lags. In such a situation, one would expect that the lags have the same sign for all the harmonics. This rules out the possibility that the lags are entirely due to a Comptonizing region surrounding the area where the QPOs are produced. The different signs demonstrate that the QPO waveform is significantly different at low photon energies with respect to that at higher energies. The same mechanism which produces the QPOs most likely also causes this difference.

Only for the black-hole transient GS 1124–683 the phase lags for low-frequency VHS QPOs have been measured before (Takizawa et al. 1997). Because we see significant differences in the results in XTE J1550–564 between different observations, it is difficult to compare the results between these two sources. The power spectrum of the 11 Jan 1991 observation of GS 1124–683 (see Fig. 3 of Takizawa et al. 1997) shows similar QPOs as in our power spectra with type B QPOs: several harmonically related QPOs with a Q of $\sim$6 for the 6 Hz QPO. The lags for the 6 Hz QPO in GS 1124–683 (between photons above 3 keV and those at 3 keV) have similar sign (hard lags) but smaller amplitudes (0.2–0.4 radian) as our type B QPOs. Another possible difference is that in GS 1124–683 also the photons below 3 keV lag the $\sim$3 keV ones. This energy range cannot accurately be probed with *RXTE*, and similar behavior cannot be excluded in XTE J1550–564. The non-detection of any lags for the noise is consistent with our results. The main difference is that for GS

1124–683 the lags have the same sign for both the 3 as the 6 Hz QPO (see Takizawa et al. 1997), while for the type B QPOs for XTE J1550–564 the signs are different. Also, during our only observation with strong band-limited noise (40401-01-57-00), the noise *and* the QPOs had soft lags, contrary to what is seen for GS1124–683. A uniform picture for the low-frequency black-hole QPOs cannot be constructed based on the results so far available.

The only other systems for which the phase lags for the low-frequency QPOs have been studied are the neutron star low-mass X-ray binaries (LMXBs). QPOs around 4–7 Hz are observed in the intrinsically brightest of these systems (van der Klis 1995), and occasionally in the lower-luminosity ones (Wijnands, van der Klis, & Rijkhorst 1998; Wijnands & van der Klis 1999; Revnivtsev et al. 1999). However, so far, no harmonics have been observed and the phase lags of these QPOs are either much larger (up to π radian; Mitsuda & Dotani 1989) or consistent with zero (e.g., Wijnands et al. 1999). The other type of low-frequency QPO seen in the neutron star LMXBs, are the 15–70 Hz QPOs. Often, two QPOs are seen which are harmonically related. Their lags are around 0.3–0.6 radian, but the hard photons always lag the soft ones (e.g., Vaughan et al. 1994), which is different from XTE J1550–564. Also, in these neutron star QPOs the amplitude of the phase lags of the fundamental is about half that of its second harmonic. In XTE J1550–564, the absolute phase lags for the different harmonics are very similar. On the basis of the lags it is doubtful if the QPOs in the neutron star LMXBs are related to the low-frequency QPOs in XTE J1550–564.

This work was supported by ASTRON (grant 781-76-017), by NOVA, and by NASA through Chandra Postdoctoral Fellowship grant number PF9-10010 awarded by CXC, which is operated by SAO for NASA under contract NAS8-39073. This research has made use of data obtained through the HEASARC Online Service, provided by the NASA/GSFC.

REFERENCES

Cui, W., Zhang, S. N., Chan, W., & Morgan, E. H. 1999, ApJ, 512, L43

Homan, J., Wijnands, R., & van der Klis, M. 1999a, IAU Circ., 7121

Homan, J., et al. 1999b, ApJ, in preparation

McClintock, J., Sobczak, G., Remillard, R., Morgan, E., Levine, A., Bailyn, C., & Orosz, J. 1998 IAU Circ., 7025

Mitsuda, K. & Dotani, T. 1989, PASJ, 41, 557

Remillard, R., Morgan, E., McClintock, J., & Sobczak, G. 1998, IAU Circ.7019

Remillard, R. A., McClintock, J. E., Sobczak, G. J., Bailyn, C. D., Orosz, J. A., Morgan, E. H., & Levine, A. M. 1999, ApJ, 517, L127

Revnivtsev, M., Borozdin, K., & Emelyanov, A. 1999, A&A, 344, L25

Smith, D. A., 1998, IAU Circ.7008

Sobczak, G. J., McClintock, J. E., Remillard, R. A., Levine, A. M., Morgan, E. H., Bailyn, C. D., Orosz, J. A. 1999, ApJ, 517, L121

Takizawa, M., Dotani, T., Mitsuda, K., Matsuba, E., Ogawa, M., Aoki, T., Asai, K., Ebisawa, K., Makishima, K, Miyamoto, S., Iga, S., Vaughan, B., Rutledge, R. E., Lewin, W. H. G. 1997, ApJ, 489, 272

van der Klis, M. 1995, In: *X-ray Binaries*, W. H. G. Lewin, J. van Paradijs, & E. P. J. van den Heuvel (eds.), Cambridge University Press, p. 252

van der Klis, M., Hasinger, G., Stella, L, Langmeier, A., van Paradijs, J., & Lewin, W. H. G. 1987, ApJ, 319, L13

Vaughan, B., van der Klis, M., Lewin, W. H. G., Wijers, R. A. M. J., van Paradijs, J., Dotani, T., & Mitsuda, K. 1994, ApJ, 421, 738

Wijnands, R. & van der Klis, 1999, ApJ, in press

Wijnands, R., van der Klis, M., & Rijkhorst, E.-J. 1999, ApJ, 512, L39

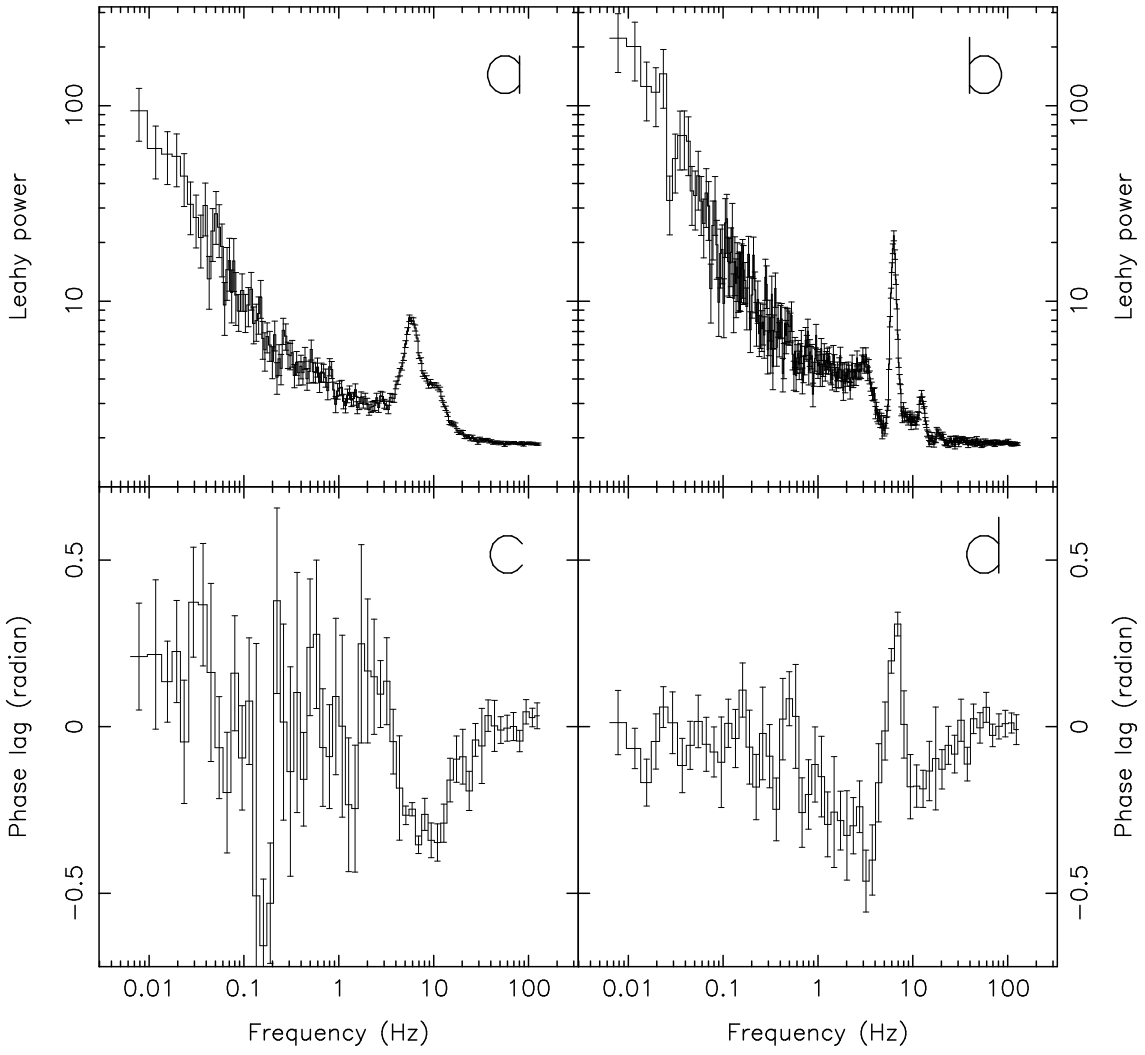

Fig. 1.— Typical Leahy normalized power spectra (2–48 keV) and phase lag spectra of observations with type A low-frequency QPOs (*a* and *c*; observation 40401-01-50-00) and of those with type B low-frequency QPOs (*b* and *d*; observation 40401-01-53-00). In *a* and *b*, the dead-time modified Poisson level has not been subtracted. The phase lag spectra (*c* and *d*) were calculated between the energy bands 2.5–6.5 and 6.5–48.0 keV. Negative phase lags mean that the soft photons lag the hard photons.

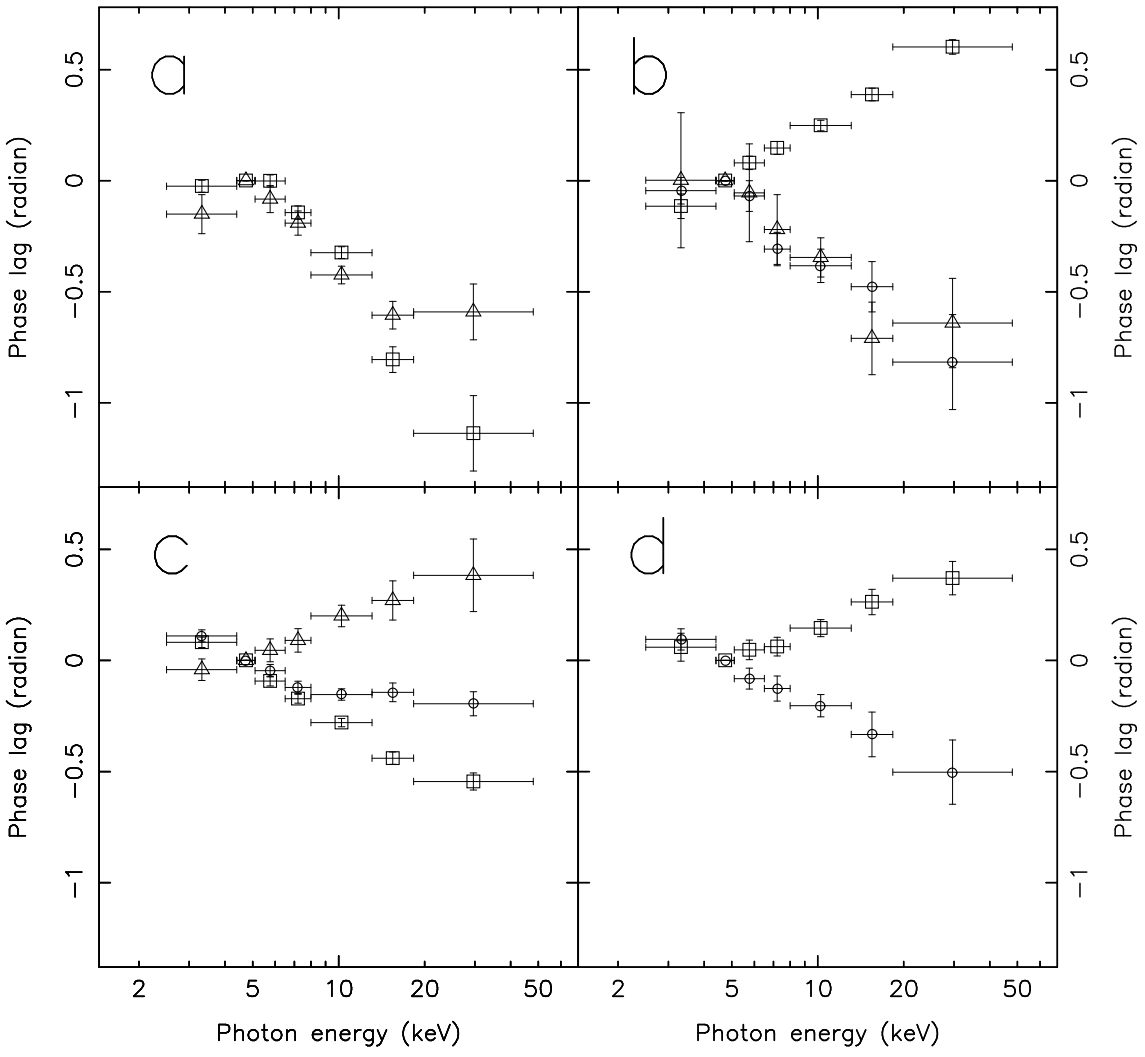

Fig. 2.— The phase lags of the 3 Hz (*open circles*), 6 Hz (*open squares*), and 12 Hz (*open triangles*) QPOs versus the photon energy of observation 40401-01-50-00 (*a*), 40401-01-53-00 (*b*), 40401-01-57-00 (*c*), and 40401-01-58-01 (*d*). The phase lags were calculated with respect to the reference energy band of 4.4–5.1 keV.

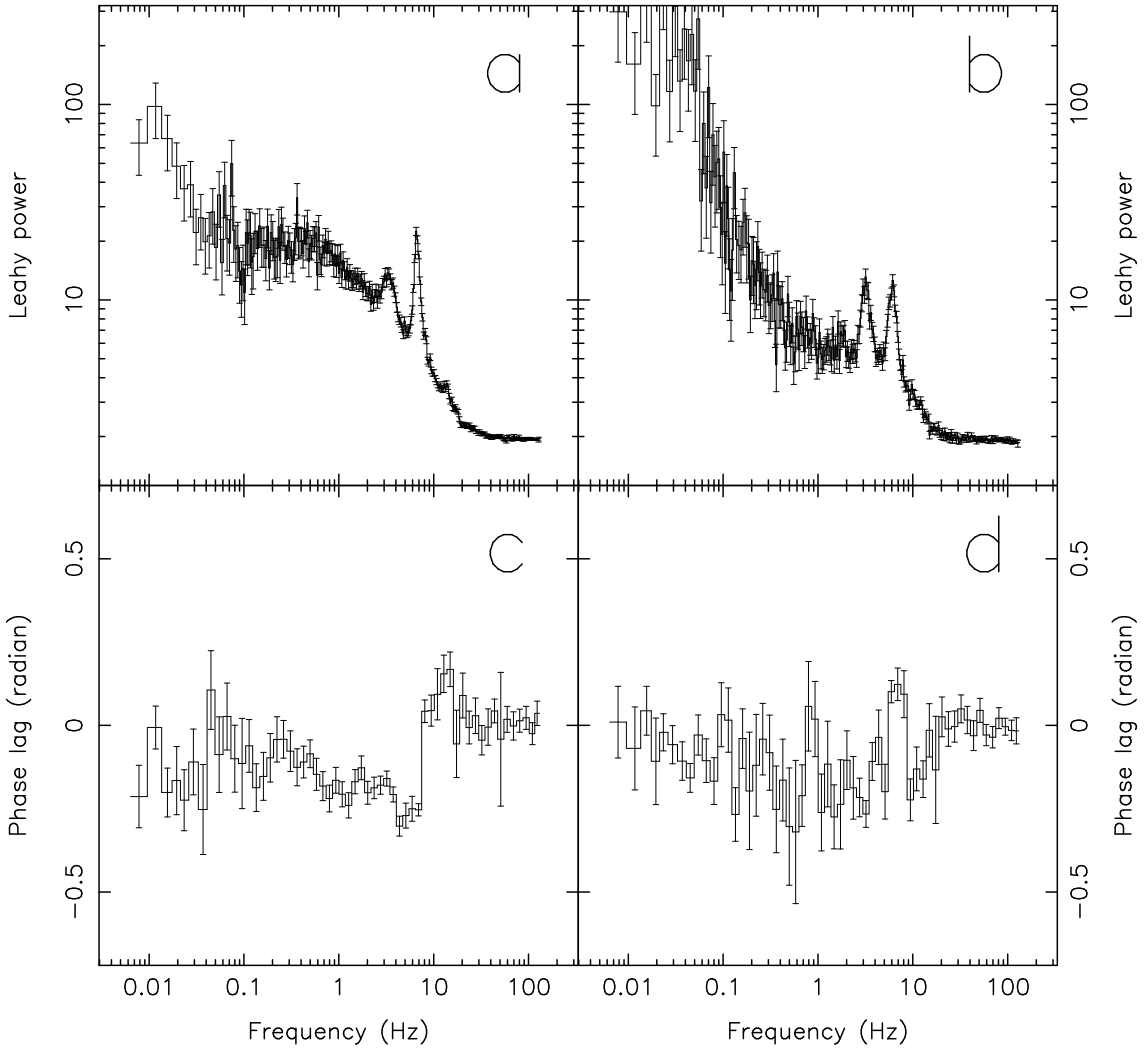

Fig. 3.— Leahy normalized power spectra (2–48 keV) of the observations 40401-01-57-00 (*a*) and 40401-01-58-01 (*b*), with their corresponding phase lag spectra (*c* and *d*, respectively). In *a* and *b*, the dead-time modified Poisson level has not been subtracted. The phase lag spectra (*c* and *d*) were calculated between the energy bands 2.5–6.5 and 6.5–48.0 keV. Negative phase lags mean that the soft photons lag the hard photons.

Table 1. A log of the observations

Type of QPO	Obs. ID	Time (March 1999; UTC)	Good Time (ksec)	Average count rate[a] counts s^{-1} ($\times 10^3$)
A	40401-01-50-00	4 19:14–20:43	3.1	20.9
	40401-01-51-00	5 12:10–13:01	1.5	20.1
	40401-01-59-01	18 02:04–02:29	1.1	11.9
	40401-01-59-00	18 03:38–05:40	4.0	11.7
	40401-01-61-01	21 02:07–02:27	0.9	9.5
	40401-01-61-00	21 11:55–12:20	1.1	9.3
B	40401-01-53-00	8 08:29–09:17	2.7	22.9
	40401-01-55-00	10 23:27–00:31	2.8	21.9
	40401-01-51-01	11 02:12–02:36	1.3	22.0
	40401-01-56-00	12 09:36–09:58	0.8	20.4
	40401-01-56-01	12 11:17–11:26	0.4	20.6
	40401-01-57-00	13 16:29–17:36	2.9	12.8
	40401-01-58-00	15 05:15–05:55	1.2	17.6
	40401-01-58-01	17 02:03–03:16	1.4	16.5

[a]The count rates are for 5 detectors on, and are background subtracted, but not dead-time corrected.